BenzoHTag, a fluorogenic self-labeling enzyme developed using molecular evolution

Bryan J. Lampkin, Benjamin J. Goldberg, and Joshua A. Kritzer*

Department of Chemistry, Tufts University, Medford MA 02155

*corresponding author: joshua.kritzer@tufts.edu

Fluorogenic dyes enable highly sensitive, real-time fluorescent readouts in live cells. Recent applications of fluorogenic dyes with self-labeling enzymes has expanded their applications, allowing high spatial and temporal resolution. However, improving fluorogenic self-labeling enzyme systems has largely focused on synthetically modifying the substrate dye and not the self-labeling enzyme. Here, we use molecular evolution to optimize the self-labeling enzyme HaloTag7 for improved performance with a designed fluorogenic substrate. Screening over 250 million variants, we isolated the optimized enzyme BenzoHTag which shows low background and rapid turn-on fluorescence in live mammalian cells.

Genetically encodable biosensors have become essential in the biochemical sciences.[1, 2] Their utility has been expanded using self-labeling enzymes, including HaloTag7,[3-5] to introduce brighter and more photostable organic dyes.[6-9] Using fluorogenic dyes is particularly appealing for cell-based assays because they provide rapid turn-on, high sensitivity, and no need for washout steps, allowing real-time monitoring of biochemical processes.[10-16] Benzothiadiazole dyes are a class of fluorogenic dyes that are non-fluorescent in aqueous solution and highly fluorescent in non-polar environments, including the HaloTag7 active site channel as demonstrated by Zhang and coworkers.[11, 17] We recently demonstrated that replacing the dimethyl amine donor in **Bz-2** with a pyrrolidine yielded **Bz-1** which had an enhanced reaction rate with HaloTag7 and 50% brighter fluorescence when conjugated to HaloTag7 (Fig. 1).[18] **Bz-1** was cell-penetrant, had low background in mammalian cells, and when conjugated to HaloTag7 **Bz-1** had spectral properties that align well with GFP and AlexaFluor488.[19, 20] Despite these improvements, the reaction rate was slower than some common HaloTag7 dye/substrates. Importantly, HaloTag7 only has rapid kinetics ($k_{app} >> 1 \times 10^4\ M^{-1}s^{-1}$) with substrates containing xanthene cores such as rhodamine or fluorescein dyes,[21, 22] which was the model substrate in the original HaloTag engineering campaign – HaloTag is no exception to the maxim "you get what you screen for." Thus, we sought to improve the fluorogenic system by modifying HaloTag7 itself. Two recent efforts have had similar goals. One produced HaloTag variants with improved fluorogenic properties when complexed with a styrylpyridium substrate, and the other produced HaloTag variants that modulated the fluorescent lifetimes of rhodamine substrates (Table S2).[23, 24] These efforts used relatively

low-throughput screening methods, picking bacterial colonies or purifying individual HaloTag variants, and were limited to screening dozens to thousands of variants.

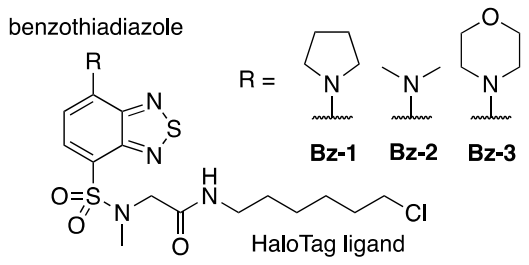

Figure 1. Fluorogenic benzothiadiazole substrates.

In this work, we use yeast surface display[25-29] to screen hundreds of millions of HaloTag variants for desirable functional properties. We cloned a codon-optimized HaloTag7 gene into the yeast display vector pCTcon2 in order to express HaloTag7 as a C-terminal Aga2 fusion with the epitope tags HA and Myc immediately C- and N-terminal to HaloTag, respectively (Fig. 2a).[30] Activity of HaloTag on the yeast surface was verified by treating yeast with chloroalkane-tetramethylrhodamine (CA-TMR) dye. Robust CA-TMR signal was observed for yeast cells expressing HaloTag7 but not cells expressing the catalytically inactive D106A mutant (Fig. S1a). Immunostaining of HA and/or Myc epitopes produced a tight linear correlation with CA-TMR signal, allowing for an estimation of the activity of HaloTag relative to expression levels (Figs. 2a,S1b). This was important to avoid bias towards high-expressing variants in subsequent screens. We used error-prone PCR to generate four sub-libraries with 2 to 6 mutations per variant (Tables S3, S4). After verifying that each sub-library retained some activity (Fig. S2) they were pooled to yield an input library of 2.5×10^8 variants. We filtered the input library to remove catalytically dead variants by treating a pool of $>4 \times 10^9$ yeast with excess chloroalkane-biotin and then isolating biotinylated yeast using magnetic streptavidin beads. This produced a filtered input library of functional HaloTag variants with up to 5×10^7 unique members.

Next, we subjected the filtered library to iterative rounds of screening using fluorescence-activated cell sorting with substrate **Bz-1**. In each round, we isolated the top 0.5% of cells with high green fluorescence relative to signal deriving from Myc expression. Stringency was increased after each round by decreasing the concentration of **Bz-1** and decreasing the incubation time, with round 4 applying 40 nM **Bz-1** for one minute (Table S6). After four rounds of screening, there was a clear increase in fluorescence of the selected variants when treated with **Bz-1** compared to HaloTag7 (Fig. 2b-c).

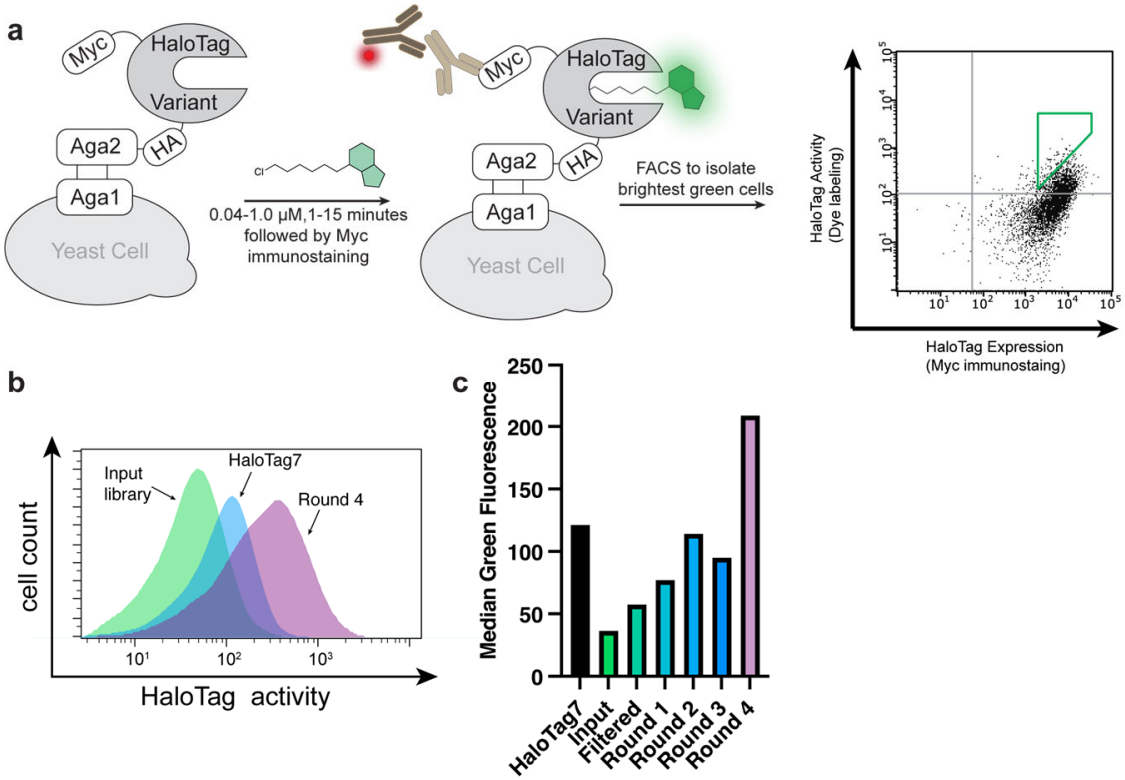

Figure 2. **Molecular evolution of a fluorogenic HaloTag system using benzothiadiazole dye Bz-1**. (a) Yeast display construct and screening strategy. Cells within the green gate were isolated and used for subsequent rounds of sorting. (b) Histograms of green fluorescence of 10,000 yeast cells displaying the input library (green), HaloTag7 (blue), or round 4 of the screen (purple). (c) Median green fluorescence of 10000 yeast cells displaying HaloTag7, the input library, the filtered input library, and the output pools of rounds 1 through rounds 4. Background green fluorescence from of unlabeled cells was subtracted out. Cells were incubated with 40nM of **Bz-1** for 1 minute.

We sequenced 110 colonies from rounds 3 and 4 and identified 15 HaloTag variants that encompassed most of the enriched mutations. Comparing the activities of these variants relative to HaloTag7 (Fig. S4 and S5, Table S7), we selected six of the best-performing variants for recombinant expression and purification – notably, most mutations were at residues that were not altered in prior, more limited HaloTag engineering efforts (Table S2). All six variants demonstrated faster labeling kinetics and brighter endpoint fluorescence intensities than HaloTag7 (Fig. 3a-c). Variant 1 produced the greatest enhancement in fluorescence intensity of **Bz-1**, which is likely due to electronic interactions between the newly introduced phenylalanine at position 246 and the benzothiadiazole core (Fig. 3d). Variants 5 and 6 had the fastest reaction rates with **Bz-1**, with over 20-fold enhancement compared to HaloTag7 (Fig. 3a). Both also produced 8% brighter fluorescence intensity than HaloTag7. These two variants shared the most-observed mutation, V245A. In a crystal structure of **Bz-2** conjugated to HaloTag,[11] V245 occupies the space directly below the core benzothiadiazole (Fig. 3d) such that a V245A mutation likely opens up space for the benzothiadiazole to alter its position within the channel. Notably, variants 2-6 all contained the V245A mutation and all showed emission maxima that were red shifted by 6 nm, further supporting a model in which the position of the benzothiadiazole has shifted. However, variants 2, 3, and 4 had reaction rates 5- to 7- fold faster

than HaloTag7, implying that the faster rates of variants 5 and 6 depended on additional contributions from their other mutations. The I211V mutation in variant 5 and the F144L mutation in variant 6 are located near the channel opening where they likely serve to widen the channel to accommodate a larger substrate (Fig. 3d).[11, 23]

We also examined the specificity of variants 5 and 6 by measuring their labeling kinetics with substrates **Bz-2** and **Bz-3**, which were characterized previously with HaloTag7 (Fig. S7).[18] Variants 5 and 6 had reaction rates with **Bz-2** and **Bz-3** that were 10-fold faster than HaloTag7 but 10-fold slower than their reaction rates with **Bz-1**. These results suggested that the selection process produced variants that were specific for both the benzothiadiazole core and the pyrrolidine substituent of **Bz-1**.

a

	Mutations	K_{app} ($M^{-1}s^{-1}$) ($x10^3$)	Percent change in fluorescence over HaloTag7	Emission Maximum (nm)
HaloTag7	–	1.5 ± 0.17	-	530
Variant 1	F144S | L246F	9.3 ± 2.0	16	530
Variant 2	V245A	11.0 ± 0.9	2	536
Variant 3	N195S | V245A | E251K | S291P	8.3 ± 1.0	11	536
Variant 4	L161W | V245A	10.3 ± 1.4	6	536
Variant 5	I211V | V245A	41.3 ± 1.6	8	536
Variant 6 (BenzoHTag)	F144L | L221S | V245A	33.4 ± 2.4	8	536

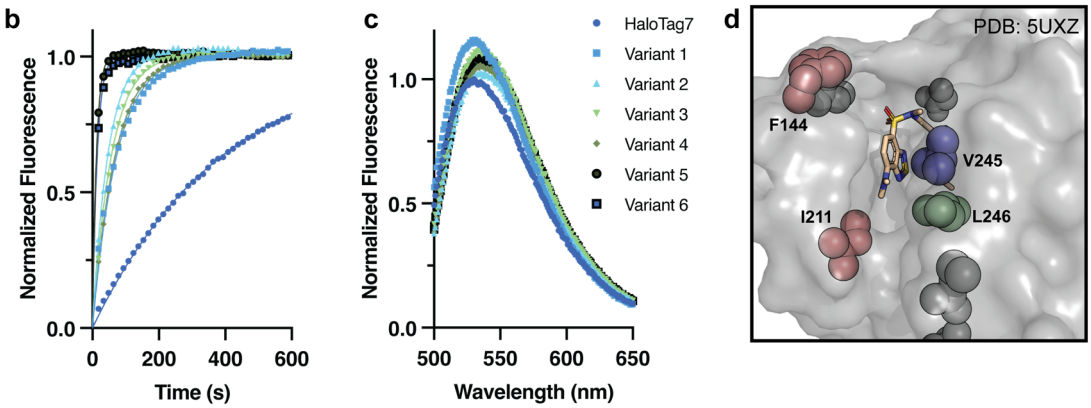

Figure 3. Characterization of recombinantly expressed HaloTag variants with improved fluorogenic properties. (a) HaloTag7 and six variants were recombinantly expressed and purified and their second-order rate constants, endpoint fluorescence intensities, and emission maxima were measured when incubated with **Bz-1**. (b) Representative kinetic traces of 0.25 μM **Bz-1** reacting with 1.0 μM HaloTag7 or selected variant. (c) Emission spectra of 2.5 μM **Bz-1** when conjugated to 5.0 μM HaloTag7 and the six variants after 2 hours of incubation, normalized to the maximum fluorescence intensity of the HaloTag7•**Bz-1** complex. (d) Crystal structure of **Bz-2** with HaloTag7 (PDB: 5UXZ)[11] showing key mutations observed in variants with improved fluorogenic properties.

We next sought to characterize the performance of fluorogenic HaloTag variant 6, which we named BenzoHTag, in live mammalian cells. BenzoHTag was cloned as a Tomm20 fusion to localize it in the cytosol attached to the outer mitochondrial membrane and the fusion was transiently transfected into U2OS cells.[24] Cells expressing BenzoHTag or HaloTag7 were treated for 10 minutes with concentrations of **Bz-1** between 7 and 500 nM (Fig. 4a). Even at the highest concentration tested, **Bz-1** showed minimal background fluorescence in non-expressing cells. BenzoHTag dramatically

outperformed HaloTag7 in live cell labeling, enabling robust fluorescence at 10- to 20-fold lower concentration of **Bz-1**. Saturation of the turn-on signal was not observed for HaloTag7-expressing cells even at 500 nM **Bz-1**, while turn-on signal saturated for BenzoHTag at 125 nM. Between 16 and 125 nM, BenzoHTag-expressing cells had 5- to 8-fold higher fluorescence over background compared to HaloTag7-expressing cells. Even after labeling for 10 minutes with only 7 nM **Bz-1**, BenzoHTag-expressing cells showed an average signal of >300-fold over background (Fig. S8).

Encouraged by these data, we evaluated the performance of the BenzoHTag•**Bz-1** system in no-wash, live cell fluorescence microscopy. U2OS cells transfected with the Tomm20-BenzoHTag fusion were treated with 30 or 10 nM **Bz-1** and imaged without exchanging media. Robust mitochondrial labeling was observed in BenzoHTag-expressing cells, which was verified by colocalization with a red mitochondrial stain (Fig. 4b), while non-expressing cells had no observable background fluorescence. We captured movies of **Bz-1**-treated cells (Movies S1, S2) and quantified the appearance of fluorescence over time. In BenzoHTag-expressing cells, **Bz-1** fluorescence approached saturation within 90 seconds of dye addition at 100 nM and at 1 nM (Fig. 4c). BenzoHTag-expressing cells saturated at 50% higher fluorescence intensities than HaloTag7-expressing cells. BenzoHTag-expressing cells with only 10 nM **Bz-1** had similar real-time labeling kinetics and intensity as HaloTag7-expressing cells with 100 nM **Bz-1** (Fig. 4c, S10). The faster labeling rate of the BenzoTag•**Bz-1** system will be especially useful for real-time monitoring of biological processes with fast time scales.[31-33]

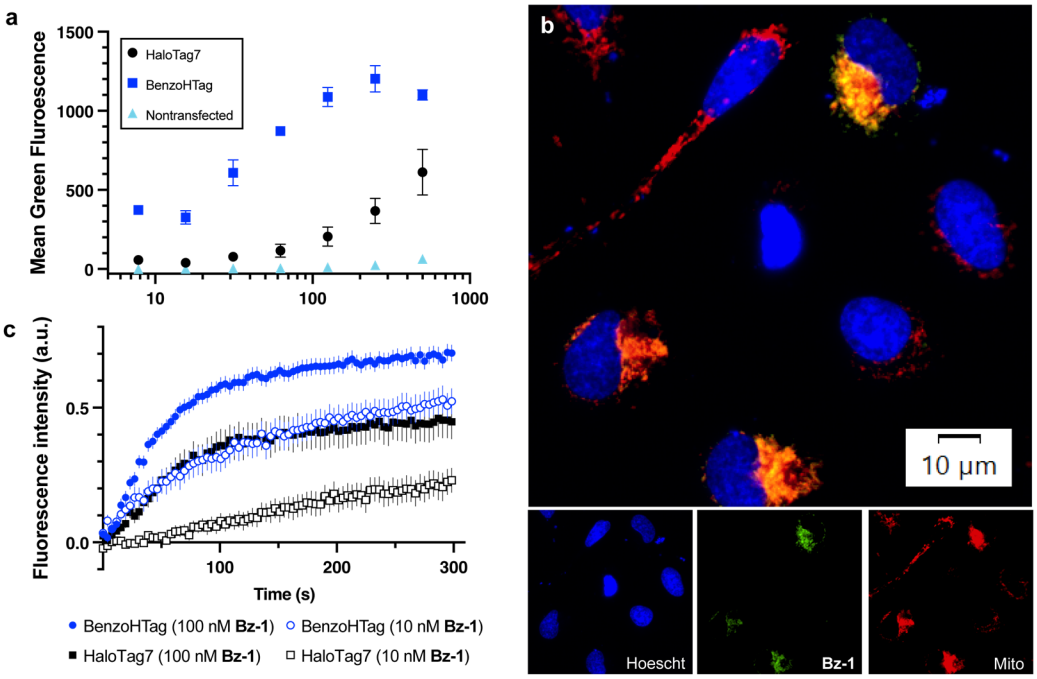

Figure 4. Bz-1 labeling in live cells. (a) Labeling with various concentrations of **Bz-1** for 10 minutes in non-transfected U2OS cells and cells transfected with BenzoHTag or HaloTag7. (b) Fluorescence microscopy imaging of Tomm20-BenzoHTag transfected U2OS cells treated with 10 nM **Bz-1**. Cells are co-stained with Hoescht and MitoLite™ Red CMXRos. (c) Growth of **Bz-1** fluorescence over time when added to U2OS cells that were transiently transfected with BenzoHTag or HaloTag7. Fluorescence intensities of >10 transfected cells for each condition were measured over the course of a five-minute video with the average background fluorescence of 10 non-transfected cells subtracted. See SI for more details.

The new BenzoHTag•**Bz-1** system has many advantageous properties. **Bz-1** is a compact, easily prepared and derivatized dye that is compatible with common blue lasers and green fluorescence emission filters. **Bz-1** has minimal background fluorescence in U2OS cells and in HeLa cells.[18] **Bz-1** forms a highly fluorescent complex with the evolved enzyme BenzoHTag, producing turn-on fluorescence in BenzoHTag-expressing cells at single-digit nanomolar concentrations of **Bz-1** after only a few seconds. We expect that these properties will make the BenzoHTag•**Bz-1** system highly translatable to a large variety of cell-based assays. For example, simply replacing HaloTag7•chloroalkane in existing assays with BenzoHTag•**Bz-1** will produce no-wash, turn-on assays for real-time monitoring of many processes in live cells including drug action at the cell surface, cell-surface receptor recycling, protein-protein interactions, targeted protein degradation, and cell penetration of peptide and oligonucleotide drugs.[31, 34-38] More broadly, the development of the BenzoHTag•**Bz-1** system highlights the power of combining creative substrate design and molecular evolution for self-labeling enzymes. This strategy is greatly accelerated by the ability to screen over 10^8 HaloTag variants at a time, rather than 10^2-10^4 as described in previous work. The yeast display system is ideal because it allows for a variety of selection formats, rapid follow-up assays, and built-in expression controls. We anticipate that this display platform can be applied to evolve many novel systems for protein labeling, biosensing, and biocatalysis that were previously inaccessible.

Acknowledgments. This work was supported by NIH 5F32GM139371 to B.L. and NIH GM148407 to J.A.K. The authors would like to thank Prof. James Van Deventer for his thoughtful insights and for providing the RJY100 yeast strain.

References

1. Greenwald, E. C.; Mehta, S.; Zhang, J., Genetically Encoded Fluorescent Biosensors Illuminate the Spatiotemporal Regulation of Signaling Networks. *Chemical Reviews* **2018,** *118* (24), 11707-11794.
2. Wang, M.; Da, Y.; Tian, Y., Fluorescent proteins and genetically encoded biosensors. *Chemical Society Reviews* **2023,** *52* (4), 1189-1214.
3. Los, G. V., et al., HaloTag: A Novel Protein Labeling Technology for Cell Imaging and Protein Analysis. *ACS Chemical Biology* **2008,** *3* (6), 373-382.
4. England, C. G.; Luo, H.; Cai, W., HaloTag Technology: A Versatile Platform for Biomedical Applications. *Bioconjugate Chemistry* **2015,** *26* (6), 975-986.
5. Cook, A.; Walterspiel, F.; Deo, C., HaloTag-Based Reporters for Fluorescence Imaging and Biosensing. *ChemBioChem* **2023,** *24* (12), e202300022.
6. Liss, V., et al., Self-labelling enzymes as universal tags for fluorescence microscopy, super-resolution microscopy and electron microscopy. *Scientific Reports* **2015,** *5* (1), 17740.
7. Erdmann, R. S., et al., Labeling Strategies Matter for Super-Resolution Microscopy: A Comparison between HaloTags and SNAP-tags. *Cell Chemical Biology* **2019,** *26* (4), 584-592.e6.
8. Deo, C., et al., The HaloTag as a general scaffold for far-red tunable chemigenetic indicators. *Nature Chemical Biology* **2021,** *17* (6), 718-723.
9. Hellweg, L., et al., A general method for the development of multicolor biosensors with large dynamic ranges. *Nature Chemical Biology* **2023,** *19* (9), 1147-1157.
10. Clark, S. A., et al., Light-Up "Channel Dyes" for Haloalkane-Based Protein Labeling in Vitro and in Bacterial Cells. *Bioconjugate Chemistry* **2016,** *27* (12), 2839-2843.
11. Liu, Y., et al., The Cation−π Interaction Enables a Halo-Tag Fluorogenic Probe for Fast No-Wash Live Cell Imaging and Gel-Free Protein Quantification. *Biochemistry* **2017,** *56* (11), 1585-1595.

12. Prifti, E., et al., A Fluorogenic Probe for SNAP-Tagged Plasma Membrane Proteins Based on the Solvatochromic Molecule Nile Red. *ACS Chemical Biology* **2014,** *9* (3), 606-612.
13. Zheng, Q., et al., Rational Design of Fluorogenic and Spontaneously Blinking Labels for Super-Resolution Imaging. *ACS Central Science* **2019,** *5* (9), 1602-1613.
14. Wang, L., et al., A general strategy to develop cell permeable and fluorogenic probes for multicolour nanoscopy. *Nature Chemistry* **2020,** *12* (2), 165-172.
15. Bachollet, S. P. J. T., et al., An expanded palette of fluorogenic HaloTag probes with enhanced contrast for targeted cellular imaging. *Organic & Biomolecular Chemistry* **2022,** *20* (17), 3619-3628.
16. Si, D., et al., Fluorogenic and Cell-Permeable Rhodamine Dyes for High-Contrast Live-Cell Protein Labeling in Bioimaging and Biosensing. *Angewandte Chemie International Edition* **2023,** *n/a* (n/a), e202307641.
17. Neto, B. A. D.; Correa, J. R.; Spencer, J., Fluorescent Benzothiadiazole Derivatives as Fluorescence Imaging Dyes: A Decade of New Generation Probes. *Chemistry – A European Journal* **2022,** *28* (4), e202103262.
18. Lampkin, B. J.; Kritzer, J., Modulating non-radiative decay pathways to improve performance of a fluorogenic HaloTag system. *Submitted* **2023**.
19. Ruhlandt, D., et al., Absolute quantum yield measurements of fluorescent proteins using a plasmonic nanocavity. *Commun Biol* **2020,** *3* (1), 627.
20. Lavis, L. D.; Raines, R. T., Bright Ideas for Chemical Biology. *ACS Chemical Biology* **2008,** *3* (3), 142-155.
21. Wilhelm, J., et al., Kinetic and Structural Characterization of the Self-Labeling Protein Tags HaloTag7, SNAP-tag, and CLIP-tag. *Biochemistry* **2021**.
22. Encell, L. P., et al., Development of a dehalogenase-based protein fusion tag capable of rapid, selective and covalent attachment to customizable ligands. *Curr Chem Genomics* **2012,** *6*, 55-71.
23. Miró-Vinyals, C., et al., HaloTag Engineering for Enhanced Fluorogenicity and Kinetics with a Styrylpyridium Dye. *ChemBioChem* **2021**.
24. Frei, M. S., et al., Engineered HaloTag variants for fluorescence lifetime multiplexing. *Nature Methods* **2021**.
25. Colby, D. W., et al., Engineering antibody affinity by yeast surface display. *Methods Enzymol* **2004,** *388*, 348-58.
26. Chen, I.; Dorr, B. M.; Liu, D. R., A general strategy for the evolution of bond-forming enzymes using yeast display. *Proceedings of the National Academy of Sciences* **2011,** *108* (28), 11399-11404.
27. Van Deventer, J. A.; Wittrup, K. D., Yeast Surface Display for Antibody Isolation: Library Construction, Library Screening, and Affinity Maturation. Humana Press: 2014; pp 151-181.
28. Branon, T. C., et al., Efficient proximity labeling in living cells and organisms with TurboID. *Nat Biotechnol* **2018,** *36* (9), 880-887.
29. Plamont, M.-A., et al., Small fluorescence-activating and absorption-shifting tag for tunable protein imaging in vivo. *Proceedings of the National Academy of Sciences* **2016,** *113* (3), 497-502.
30. Chao, G., et al., Isolating and engineering human antibodies using yeast surface display. *Nat Protoc* **2006,** *1* (2), 755-68.
31. Jonker, C. T. H., et al., Accurate measurement of fast endocytic recycling kinetics in real time. *Journal of Cell Science* **2020,** *133* (2).
32. Komatsu, T., et al., Real-Time Measurements of Protein Dynamics Using Fluorescence Activation-Coupled Protein Labeling Method. *Journal of the American Chemical Society* **2011,** *133* (17), 6745-6751.
33. Sahni, A.; Qian, Z.; Pei, D., Cell-Penetrating Peptides Escape the Endosome by Inducing Vesicle Budding and Collapse. *ACS Chemical Biology* **2020,** *15* (9), 2485-2492.
34. Shields, B. C., et al., Deconstructing behavioral neuropharmacology with cellular specificity. *Science* **2017,** *356* (6333), eaaj2161.
35. Machleidt, T., et al., NanoBRET—A Novel BRET Platform for the Analysis of Protein–Protein Interactions. *ACS Chemical Biology* **2015,** *10* (8), 1797-1804.
36. Buckley, D. L., et al., HaloPROTACS: Use of Small Molecule PROTACs to Induce Degradation of HaloTag Fusion Proteins. *ACS Chem Biol* **2015,** *10* (8), 1831-7.
37. Deprey, K., et al., Quantitative Measurement of Cytosolic and Nuclear Penetration of Oligonucleotide Therapeutics. *ACS Chemical Biology* **2022,** *17* (2), 348-360.
38. Peraro, L., et al., Cell Penetration Profiling Using the Chloroalkane Penetration Assay. *Journal of the American Chemical Society* **2018,** *140* (36), 11360-11369.